Immunolocalization of anion exchanger AE2 and Na^+-HCO_3^- cotransporter in rat parotid and submandibular glands

ELENI ROUSSA,[1] MICHAEL F. ROMERO,[2] BERNHARD M. SCHMITT,[3] WALTER F. BORON,[3] SETH L. ALPER,[4] AND FRANK THÉVENOD[1]

[1]Departments of Anatomy and [5]Physiology, Medical Faculty, University of Saarland, 66421 Homburg/Saar, Germany; [2]Department of Physiology and Biophysics and Department of Pharmacology, Case Western Reserve University School of Medicine, Cleveland, Ohio 44106-4790; [3]Department of Cellular and Molecular Physiology, Yale University School of Medicine, New Haven, Connecticut 06520; and [4]Molecular Medicine and Renal Units, Beth Israel Deaconess Medical Center and Department of Cell Biology, Harvard Medical School, Boston, Massachusetts 02215

Roussa, Eleni, Michael F. Romero, Bernhard M. Schmitt, Walter F. Boron, Seth L. Alper, and Frank Thévenod. Immunolocalization of anion exchanger AE2 and Na^+-HCO_3^- cotransporter in rat parotid and submandibular glands. *Am. J. Physiol.* 277 (*Gastrointest. Liver Physiol.* 40): G1288–G1296, 1999.—Salivary glands secrete K^+ and HCO_3^- and reabsorb Na^+ and Cl^-, but the identity of transporters involved in HCO_3^- transport remains unclear. We investigated localization of Cl^-/HCO_3^- exchanger isoform AE2 and of Na^+-HCO_3^- cotransporter (NBC) in rat parotid gland (PAR) and submandibular gland (SMG) by immunoblot and immunocytochemical techniques. Immunoblotting of PAR and SMG plasma membranes with specific antibodies against mouse kidney AE2 and rat kidney NBC revealed protein bands at ~160 and 180 kDa for AE2 and ~130 kDa for NBC, as expected for the AE2 full-length protein and consistent with the apparent molecular mass of NBC in several tissues other than kidney. Immunostaining of fixed PAR and SMG tissue sections revealed specific basolateral staining of PAR acinar cells for AE2 and NBC, but in SMG acinar cells only basolateral AE2 labeling was observed. No AE2 expression was detected in any ducts. Striated, intralobular, and main duct cells of both glands showed NBC expression predominantly at basolateral membranes, with some cells being apically stained. In SMG duct cells, NBC staining exhibited a gradient of distribution from basolateral localization in more proximal parts of the ductal tree to apical localization toward distal parts of the ductal tree. Both immunoblotting signals and immunostaining were abolished in preabsorption experiments with the respective antigens. Thus the mechanisms of fluid and anion secretion in salivary acinar cells may be different between PAR and SMG, and, because NBC was detected in acinar and duct cells, it may play a more important role in transport of HCO_3^- by rat salivary duct cells than previously believed.

bicarbonate transport; ducts; acini; secretion

SALIVA FORMATION is a two-stage process (37). Primary saliva, a plasma-like isotonic fluid, is secreted by acinar secretory end pieces and undergoes modification of its ionic composition in the duct system. On the basis of the anion composition of the primary fluid, salivary glands can be divided into two groups: those producing a Cl^--rich primary saliva, such as the rat parotid and submandibular glands, and those producing a HCO_3^--rich primary saliva, such as sheep parotid (8, 24, 33). Agonist-induced secretion of Cl^--rich primary saliva by acinar cells is driven by the parallel operation of a basolaterally located Na^+-K^+-ATPase, a Na^+-K^+-$2Cl^-$ cotransporter (and/or coupled Na^+/H^+ and Cl^-/HCO_3^- exchangers), and a K^+ channel together with an apically located Cl^- channel (8, 20). In contrast, stimulated secretion of HCO_3^--rich primary saliva by the sheep parotid appears to be driven by basolateral Na^+-HCO_3^- cotransport and HCO_3^- efflux across the apical membrane via a HCO_3^- conductance (24, 33).

The ducts modify the electrolyte composition of the primary saliva with little or no further net water movement to produce the hypotonic final saliva. Luminally located Na^+ and Cl^- channels, Na^+/H^+, K^+/H^+, and Cl^-/HCO_3^- exchangers, together with the basolaterally located Na^+-K^+-ATPase, K^+ and Cl^- channels, and additional Na^+/H^+ exchangers are thought to be involved in ductal electrolyte transport, resulting in secretion of K^+ and HCO_3^- and reabsorption of Na^+ and Cl^- (8, 12, 13).

Which transporters could mediate HCO_3^- transport at the molecular level? A family of band 3-related anion exchanger (AE) gene products has been cloned that functionally mediates Cl^-/HCO_3^- exchange. It consists of three members, AE1, AE2 and AE3, which are expressed in a variety of tissues (2). AE1 (or band 3) (15) is the major protein of erythrocyte plasma membranes and of type A intercalated cells of the renal cortical collecting duct. AE2 is expressed in many epithelia, including kidney, gastric parietal cells, intestine, biliary tree, and genitourinary tract (2, 3, 4, 5, 11). AE3 has been detected in the nervous system (bAE3) (14) and cardiac muscle (cAE3) (44), as well as in the gut (16). The Cl^-/HCO_3^- exchangers belong to a superfamily of bicarbonate transporters (26), which also includes the recently cloned Na^+-HCO_3^- cotransporters (1, 25, 27, 28), a K^+-HCO_3^- cotransporter, and a Na^+-driven Cl^-/HCO_3^- exchanger.

So far, little is known about the molecular identity of the transporters involved in HCO_3^- secretion by salivary acinar and duct cells. Although some functional data support the presence of Cl^-/HCO_3^- exchangers in rat submandibular ducts (8, 12, 13, 46) and rat parotid acini (20), the identity and distribution of AE isoforms

The costs of publication of this article were defrayed in part by the payment of page charges. The article must therefore be hereby marked "*advertisement*" in accordance with 18 U.S.C. Section 1734 solely to indicate this fact.

 0193-1857/99 $5.00

expressed in salivary glands are still unclear (10, 42). Functional studies in sheep parotid glands (24, 33) have suggested a role for a Na^+-HCO_3^- cotransporter in HCO_3^- secretion by salivary glands. This is supported by recent studies in another exocrine gland, the exocrine pancreas, in which the Na^+-HCO_3^- cotransporter (NBC) was found to be expressed in both acinar and duct cells (1, 39). The aim of the present study was therefore to investigate protein expression and localization of AE2 and NBC in rat parotid and submandibular gland by immunoblotting of subcellular membrane fractions and by immunofluorescence and immunoperoxidase light microscopy of fixed tissue sections with specific polyclonal antibodies to the transporters. The results indicate the presence of AE2 and NBC in rat salivary glands. AE2 is located basolaterally in acinar cells of both parotid and submandibular glands and is absent from duct cells in both glands. NBC is basolaterally expressed in parotid acinar cells but undetectable in submandibular acinar cells. Duct cells of both glands express NBC at their basolateral membranes, with some duct cells also exhibiting apical staining. In addition, in submandibular duct cells NBC staining shifts to a predominant apical localization in the distal parts of the duct tree.

MATERIALS AND METHODS

Antibodies

An affinity-purified rabbit polyclonal antibody to the COOH-terminal amino acids (aa) 1224–1237 of mouse AE2 (aAE2-CT) has been previously described (34). Generation and specificity of the rabbit polyclonal anti-[maltose binding protein (MBP)-NBC3] serum raised against rat kidney NBC (rkNBC) NH_2-terminal aa 338–391 and anti-(MBP-NBC5) serum raised against rkNBC COOH-terminal aa 928–1035 have been reported earlier (31). A horseradish peroxidase-conjugated goat anti-rabbit IgG (DAKO) and a donkey anti-rabbit IgG coupled to indocarbocyanin (Dianova, Hamburg, Germany) were used as secondary antibodies. For competition experiments with the anti-AE2-COOH-terminal (CT) antibody, either a mouse AE2 COOH-terminal peptide (aa 1224–1237) or a mouse AE1 COOH-terminal peptide (aa 917–929) were used. For competition experiments with the anti-NBC antibodies, the respective fusion proteins were used with MBP as control. All competition experiments were carried out by preabsorbing primary antibodies with the respective antigens for 2 h before application of the antibodies.

Tissue Preparation for Light Microscopy

Male Wistar rats were anesthetized with pentobarbital sodium (Nembutal, 65 mg/kg ip) and perfusion-fixed with 2% paraformaldehyde-75 mM lysine-10 mM sodium periodate (PLP) as described by McLean and Nakane (18). Parotid and submandibular glands were removed, cut into blocks, and further fixed in fresh fixative overnight at 4°C. PLP-fixed tissue was washed four times for 10 min with PBS and kept in PBS containing 0.02% sodium azide at 4°C until further use.

Dependence of Immunolabeling on Tissue Fixation, Processing, and Epitope Unmasking With SDS

The localization of AE2 in rat parotid and submandibular glands was examined by immunohistochemistry using the affinity-purified rabbit polyclonal antibody to the COOH-terminal aa 1224–1237 of mouse AE2. Detection and pattern of immunoreactivity appeared to depend on tissue fixation, processing for immunohistochemistry, and/or epitope unmasking procedure with SDS. This antibody detected specific immunostaining only in cryosections obtained from PLP-fixed tissue, and impressive effects on detection as well as on distribution of this AE2 epitope were observed using epitope "unmasking," i.e., by treating the sections with 1% SDS for 5 min, as described below. In contrast to the antibody against AE2, both antibodies used in the present study for detection of NBC epitopes did not appear to be fixation sensitive. In addition, treating the fixed tissue sections with 1% SDS for 5 min enhanced NBC immunolabeling but did not alter NBC staining pattern in rat parotid and submandibular glands.

Immunofluorescence and Immunoperoxidase Light Microscopy on Cryosections

Tissue blocks were cryoprotected in 30% sucrose for at least 1 h and frozen in liquid N_2. Indirect immunohistochemistry was performed on 5-μm cryosections. Sections were rehydrated in PBS for 5 min, blocked with 1% BSA-PBS for 15 min, and incubated with primary antibodies at dilutions of 1:800 for the aAE2-CT and of 1:400 for both NBC antibodies in PBS containing 0.02% sodium azide overnight at 4°C. Epitope unmasking with SDS was also performed on some sections, as reported by Brown et al. (7). Briefly, after rehydrating in PBS, sections were treated with 1% SDS for 5 min and washed three times with PBS for 5 min before blocking with 1% BSA-PBS. After incubation with the primary antibody, slides were washed three times with PBS for 5 min and incubated with donkey anti-rabbit IgG coupled to indocarbocyanin (1:600 dilution) for 1 h at room temperature. Sections were washed three times with PBS for 5 min and mounted with 2:1 Vectashield-0.1 M Tris·HCl (pH 8.0). Labeled sections were examined using an Olympus BX50F microscope equipped with a ×40 Olympus UPlanFl objective and a narrow-band green fluorescence exciter filter (wavelength 530–550 nm). Images were recorded with a three charge-coupled device color video camera (Sony DXC-950) and were digitized to 8 bits/pixel using a software developed in the laboratory. Digitized images were processed for documentation using Adobe Photoshop D1-4.0 software (Herzogenaurach, Germany). For immunoperoxidase light microscopy, sections were treated as described above until the incubation step with primary antibodies. Slides were then washed three times with PBS for 5 min and incubated with goat anti-rabbit IgG horseradish peroxidase-conjugated antibody (1:50 dilution) for 1 h at room temperature. Slides were washed three times with PBS for 5 min, and peroxidase activity was visualized with diaminobenzidine and hydrogen peroxide. Sections were dehydrated in a graded series of ethanol concentrations (70%, 80%, 90%, 96%, and 100%), cleared in xylene, and mounted with DePeX mounting medium. Labeled sections were examined with a light microscope (Olympus, Tokyo, Japan). Images were recorded with charge-coupled device cameras connected to a frame grabber that was mounted in an IBM-compatible personal computer.

Preparation of Glandular Tissue Homogenate and Isolation of Plasma Membranes

Four to six male Wistar rats were anesthetized with ether and perfused via the left ventricle with PBS until the salivary glands were thoroughly blanched. Subcellular fractionation

of parotid and submandibular glands was performed essentially as described earlier (40). Briefly, parotid or submandibular gland homogenate was prepared by grinding tissue with 50 strokes of a motor-driven Potter homogenizer in 10 ml of ice-cold homogenizing buffer containing (in mM) 280 mannitol, 10 HEPES, 10 KCl, 1 $MgCl_2$ (pH 7.0), and 0.1 Pefabloc SC (Boehringer Mannheim). The homogenate was centrifuged at 50 *g* for 5 min, and the supernatant was collected. The pellet containing unbroken cells was resuspended in 10 ml of the same buffer and homogenized once more. After centrifugation at 50 *g* for 5 min, both supernatants were combined. To obtain plasma membrane fractions, the cleared homogenate was centrifuged for 12 min at 1,000 *g* and the supernatant was centrifuged at 11,000 *g* for 15 min. The 11,000-*g* pellet was composed of an whitish fluffy upper layer and a yellowish bottom layer, which were separated. The 11,000-*g* fluffy layer was mixed with 2.0 M sucrose buffer to a concentration of 1.25 M, which was layered on 2.0 M sucrose and overlaid with 0.3 M sucrose. The gradient was centrifuged at 140,000 *g* for 90 min, and the whitish band enriched in plasma membranes (PM) at the upper surface between the 0.3 M and 1.25 M sucrose density layers was collected. Protein concentration was assayed as described by Bradford (6), using BSA as a standard.

SDS-PAGE and Western Blotting

Electrophoresis and blotting procedures were performed essentially as described earlier (38). Briefly, proteins were separated by SDS-PAGE on 7.5% acrylamide Laemmli minigels and transferred onto polyvinylidene difluoride membranes (Dupont NEN, Bad Homburg, Germany). The efficiency of protein transfer was monitored with prestained protein standards (Bio-Rad, Munich, Germany). Blots were blocked with 3% nonfat dry milk in Tris-buffered saline containing 0.05% Tween 20 for 8 h at 4°C and incubated with the primary antibodies at dilutions 1:10,000 for the aAE2-CT and 1:500 for both anti-NBC antibodies at 4°C overnight. After incubation with horseradish peroxidase-conjugated secondary antibody (1:10,000 dilution donkey anti-rabbit IgG; Amersham-Buchler, Braunschweig, Germany), blots were developed in enhanced chemiluminescence reagents (Amersham-Buchler) and signals were visualized on X-ray films. X-ray films were scanned with a single-pass flat-bed scanner (Linotype-Hell, Eschborn, Germany) and processed for documentation using JASC Paint Shop Pro 4.1 software (Jameln, Germany).

RESULTS

Immunoblotting

Immunoblotting was performed in whole parotid or submandibular gland tissue homogenate and additionally in the respective plasma membrane fraction, because both the Cl^-/HCO_3^- exchanger and Na^+-HCO_3^- cotransporter are plasma membrane transporters and are therefore expected to be enriched in purified plasma membranes.

AE2. Figure 1*A* shows an immunoblot of whole parotid or submandibular gland homogenate and PM fractions with the anti-AE2-CT antibody (1:10,000). With anti-AE2-CT, a band of ~95 kDa was labeled in the parotid homogenate fraction, whereas in the submandibular gland homogenate no bands were detectable. In the PM fractions of both glands, this antibody recognized major bands at ~100 kDa, ~110 kDa, and ~160 kDa and a faint band at ~180 kDa. The ~180-kDa and ~160-kDa bands were more prominent in

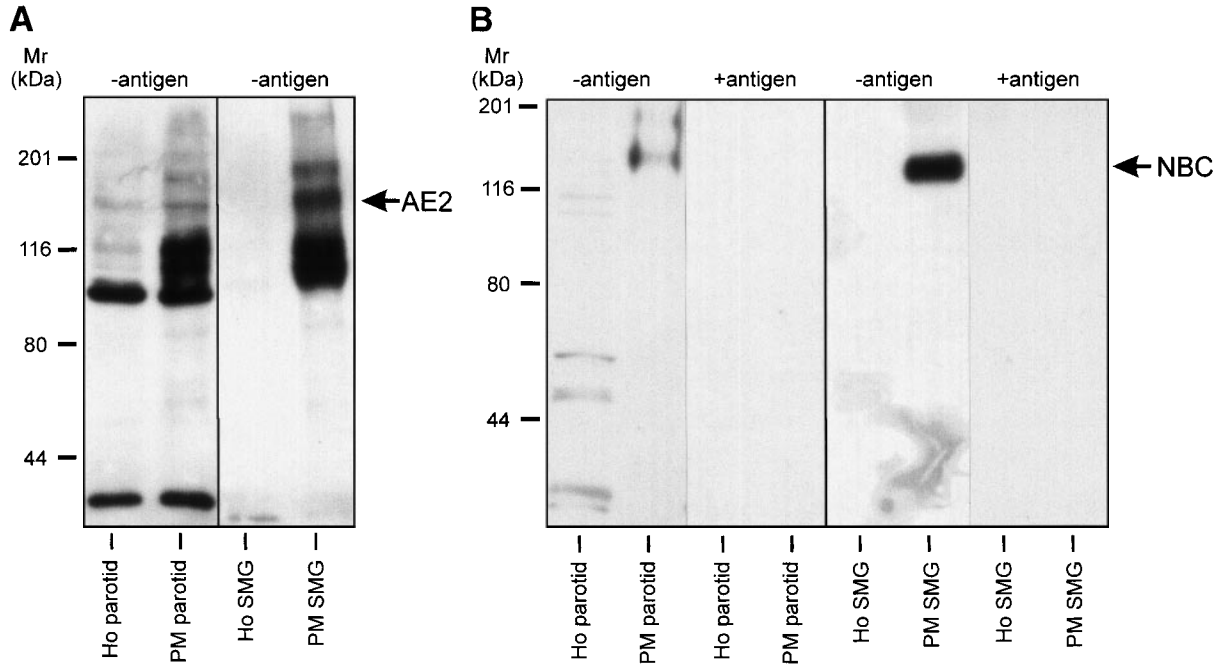

Fig. 1. Immunoblot analysis of rat parotid and submandibular glands (SMG) with polyclonal antibodies against anion exchanger (AE2) or Na^+-HCO_3^- cotransporter (NBC). Thirty micrograms of whole parotid or submandibular gland homogenate (Ho) or of plasma membrane fractions (PM) were separated by SDS-PAGE and immunoblotted either with the anti-AE2 amino acids (aa) 1224–1237 antibody (1:10,000) (*A*), with the anti-(MBP-NBC5) antibody (submandibular; 1:1,000) or with the anti-(MBP-NBC3) antibody (parotid; 1:1,000) (*B*). Antibodies were used in the absence (−antigen) or presence (+antigen) of 10 μg/ml fusion protein. One representative blot of 3 experiments is shown. M_r, apparent molecular mass.

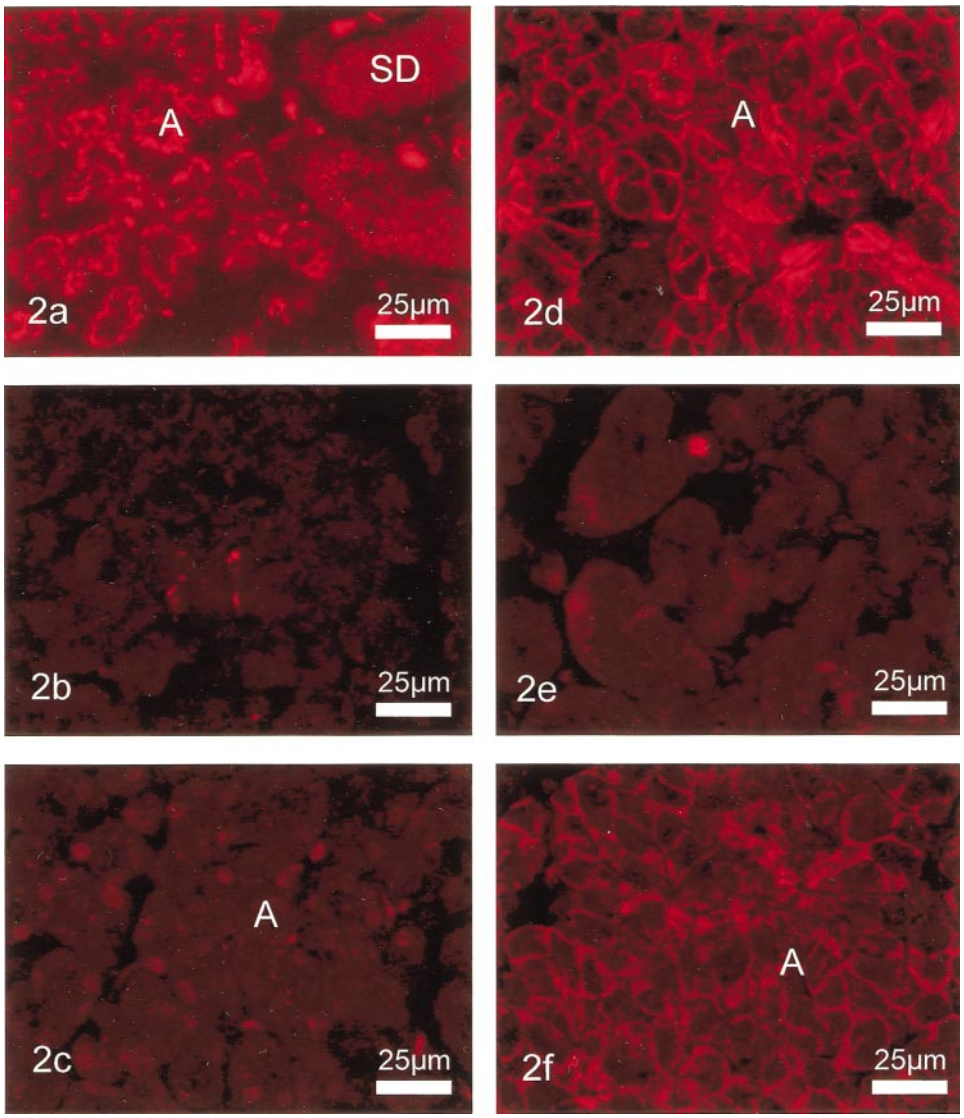

Fig. 2. Immunostaining of rat parotid gland with anti-AE2 aa 1224–1237 antibody (aAE2-CT; 1:800 dilution). Immunofluorescence light microscopy on SDS-untreated (*a–c*) and SDS-treated (*d–f*) 5-μm fixed cryosections. AE2 labeling in acinar (A) and striated duct (SD) cells is shown. In *a* and *d*, no peptide antigen was added; in *b* and *e*, sections were labeled with aAE2-CT that had been preabsorbed with 24 μg/ml AE2-CT peptide antigen. *c* and *f*: Incubation of sections with aAE2-CT antibody and 12 μg/ml AE1-CT peptide antigen. Experiment shown is representative of 20 independent experiments from 10 animals.

the submandibular than in the parotid plasma membranes. All signals probed with the aAE2-CT antibody in the immunoblots were abolished when this antibody was preincubated with 2.4 μg/ml AE2 peptide antigen (data not shown).

NBC. The results of immunoblotting experiments with NBC antisera (1:1,000) on homogenate and PM fraction of whole rat parotid [anti-(MBP-NBC3)] and submandibular gland [anti-(MBP-NBC5)] are shown in Fig. 1*B*. Similar results were obtained in the two glands with both antibodies. A prominent band of ~130 kDa was detected in the plasma membrane fraction of both glands that was not found in the respective homogenate. Labeling of these bands was abolished by preabsorption of the antibody with an excess concentration (10 μg/ml) of the respective fusion protein.

Immunohistochemistry

The duct system of rat submandibular gland can be morphologically divided into four segments. The intercalated ducts are short and narrow duct segments that form the most proximal part of the duct tree. They drain into the granular ducts, which are well developed in submandibular glands of male rodents. Granular ducts consist of three cell types: the wide dark granular cells, the light granular cells, and the narrow agranular cells (36). The distal parts of granular ducts form the striated ducts, which are characterized by extensive infoldings of their basal membranes surrounded by many mitochondria. Striated ducts lead to nonstriated interlobular or excretory ducts. In contrast to the rat submandibular duct system, the duct system of the parotid gland is characterized by longer intercalated ducts and the absence of granular ducts (32, 36, 45).

AE2 in parotid gland. Figure 2*a* shows the labeling pattern on cryosections of PLP-fixed parotid gland with the aAE2-CT antiserum (dilution 1:800) using immunofluorescence light microscopy. In acinar cells, staining by this AE2 antibody was found to be intracellular and of moderate to strong intensity. However, labeling was not diffusely distributed throughout the cytoplasm but appeared particulate, suggesting AE2 immunoreactiv-

ity in the Golgi apparatus, as shown at the ultrastructural level in rat and mouse kidney (4, 35), but its identity and function remain unclear. Intercalated duct cells showed a faint diffuse intracellular staining pattern, whereas in striated ducts labeling was weak or absent. Labeling of the parenchyma was nearly completely abolished in the presence of the aAE2-CT peptide (24 μg/ml) (Fig. 2*b*).

The effect of 1% SDS pretreatment on immunostaining with the aAE2-CT antibody in cryostat sections of rat parotid gland is shown in Fig. 2*d*. This epitope unmasking procedure altered the immunostaining pattern in acinar cells but not in duct cells. Acinar cells showed sharp staining clearly restricted to the basolateral cell surface, whereas the Golgi-like immunostaining pattern found without SDS pretreatment was abolished. Acinar cell labeling was abolished by coincubation with the peptide antigen (24 μg/ml) (Fig. 2*e*). Because the aAE2-CT antibody cross-reacts with the COOH-terminal sequence of AE1, additional experiments were performed to distinguish between AE2 and AE1 labeling. First, peptide competition experiments were performed using the AE1-CT peptide. Figure 2*c* shows that, on sections not pretreated with SDS, coincubation of aAE2-CT with the AE1-CT peptide antigen (12 μg/ml) eliminated acinar Golgi-like staining, as previously described for rat (5) and mouse (35) kidney. In contrast, in sections pretreated with SDS (Fig. 2*f*), preabsorption with AE1-CT peptide via the same protocol minimally affected acinar basolateral staining, indicating that basolateral staining is AE2 specific.

NBC in parotid gland. Figure 3 shows NBC localization in PLP-fixed cryosections of rat parotid gland using the anti-(MBP-NBC5) antibody and immunoperoxidase light microscopy. Identical labeling pattern was obtained using the anti-(MBP-NBC3) antibody (data not shown). Staining intensity obtained with both antibodies was enhanced by treating the sections with SDS. Acinar cells uniformly exhibited basolateral immunostaining of moderate intensity, presumably representing labeling of the basolateral plasma membrane (Fig. 3*a*). Labeling in intercalated ducts was diffusely intracellular, whereas striated duct cells showed NBC immunolabeling of strong intensity at their basolateral cell sides (Fig. 3*a*). However, cells exhibiting intracellular labeling were also observed. Moreover, although basolateral staining was present in all cells lining the striated ducts, some cells were labeled at both apical and basolateral membranes (Fig. 3*a*). NBC distribution in intralobular, interlobular, and main duct cells was the same as in striated duct cells (Fig. 3*b*). Both acinar and duct staining were abolished in competition experiments with 10 μg/ml fusion protein, as shown in Fig. 3*c*.

AE2 in submandibular gland. Figure 4 shows AE2 distribution in cryosections of PLP-fixed submandibular gland tissue with the antibody aAE2-CT (dilution 1:800). In sections that had not been pretreated with SDS, submandibular acinar cells (Fig. 4*a*) showed Golgi-like staining similar to that found in parotid gland (see also Fig. 2*a*). Staining was weak or absent in granular and striated duct cells and never detectable in intercalated duct cells. Labeling of acinar cells was abolished when the aAE2-CT antibody was coincubated with its peptide antigen (24 μg/ml; Fig. 4*b*).

Epitope unmasking with SDS affected AE2 labeling in acinar cells of the submandibular gland in a similar way as in parotid glands. After incubation with the aAE2-CT, acinar cells showed staining at the basolat-

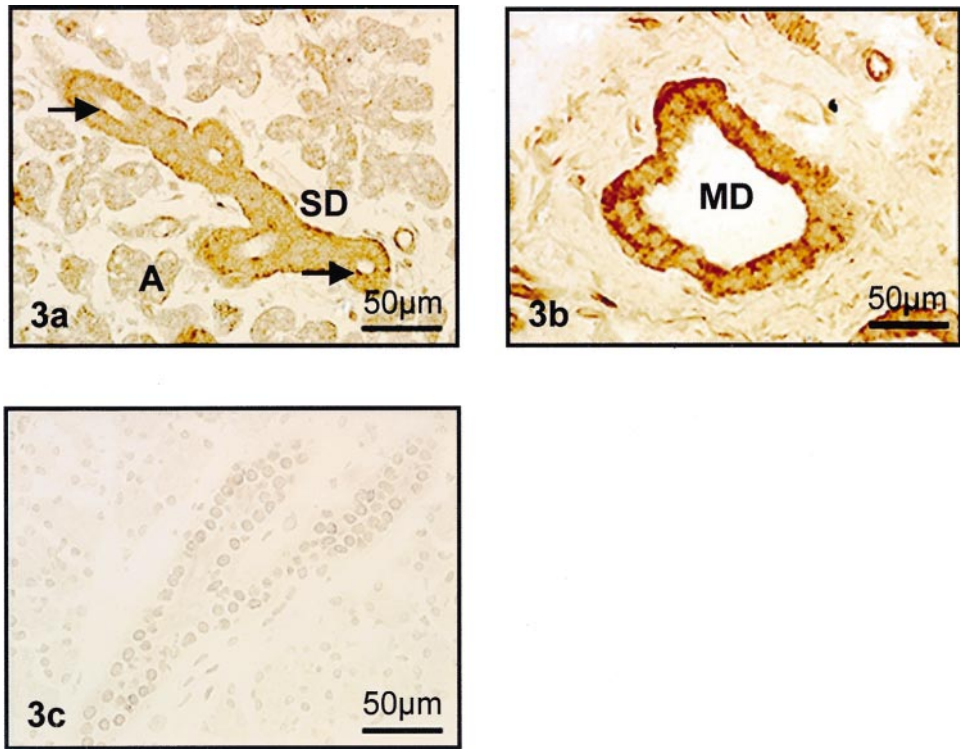

Fig. 3. Staining of NBC in rat parotid gland with anti-(MBP-NBC5) antibody (1:400 dilution) by immunoperoxidase light microscopy. *a*: NBC immunostaining in acinar (A) and striated duct (SD) cells. Arrows indicate duct cells displaying basolateral and apical staining. *b*: NBC distribution in main duct (MD) cells is shown. *c*: Incubation of the sections with anti-(MBP-NBC5) antibody in presence of excess fusion protein (10 μg/ml). Representative sections of 20 similar sections are shown.

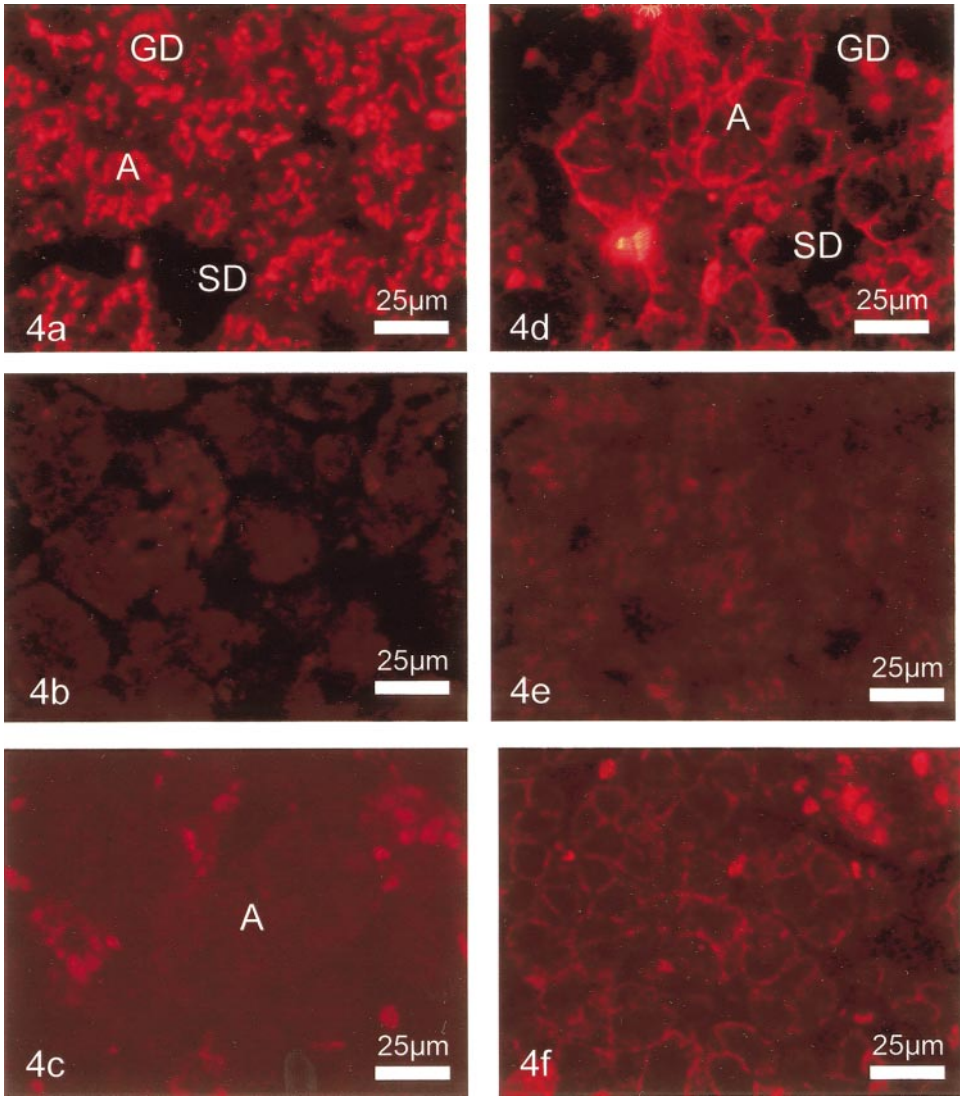

Fig. 4. Cellular distribution of AE2 in rat submandibular gland using aAE2 COOH-terminal aa 1224–1237 antibody (aAE2-CT; 1:800 dilution). Immunofluorescence light microscopy was carried out on 5-μm fixed cryosections without (*a–c*) and with (*d–f*) SDS treatment. AE2 immunostaining in acinar (A), granular duct (GD), and striated duct (SD) cells is shown. In *a* and *d*, no peptide antigen was added; in *b* and *e*, sections were labeled with aAE2-CT that had been preabsorbed with 24 μg/ml AE2-CT peptide antigen. *c* and *f*: Incubation of sections with aAE2-CT antibody in presence of 12 μg/ml AE1-CT peptide antigen is shown. Representative images of 10 experiments from 5 animals are shown.

eral cell side, and the Golgi-like staining of acinar cells found in sections without SDS pretreatment disappeared (Fig. 4*d*). When the aAE2-CT antibody was preabsorbed with its peptide antigen, staining was abolished (Fig. 4*e*). To determine the labeling specificity (AE2 or AE1), similar peptide competition experiments were performed as for parotid gland. In sections with SDS pretreatment, AE1-CT peptide (12 μg/ml) coincubated with aAE2-CT reduced but did not abolish acinar basolateral staining (Fig. 4*f*). In sections that had not been pretreated with SDS (Fig. 4*c*), acinar Golgi staining was abolished by coincubation of aAE2-CT with AE1-CT peptide.

NBC in submandibular gland. Figure 5 illustrates the labeling pattern of fixed cryosections with the anti-(MBP-NBC3) antibody. As observed in the parotid gland, both anti-NBC antibodies revealed identical immunostaining patterns in submandibular gland. However, in contrast to parotid gland, NBC immunoreactivity was absent in acinar and intercalated duct cells (Fig. 5*a*). Granular and striated duct cells showed uniform basolateral NBC immunolabeling of moderate to strong intensity with only occasional individual cells exhibiting apical staining (Fig. 5*a*). Interestingly, the number of duct cells showing apical NBC staining increased at the distal part of the submandibular duct tree. Most intralobular and interlobular duct cells revealed basolateral NBC immunostaining (Fig. 5*c*), whereas, as can be seen from Fig. 5, *b* and *d*, in the main duct cell, labeling was diffuse, with a predominance at the apical membrane. Again, labeling was abolished in the presence of 10 μg/ml fusion protein but not in the presence of MBP alone (data not shown).

DISCUSSION

Protein Expression of AE2 and NBC in Salivary Glands

AE2. With the use of specific antibodies, the presence of AE2 and NBC in rat salivary glands was first demonstrated in a plasma membrane fraction by immunoblotting (other subcellular fractions did not show any enrichment of the AE2 and NBC protein bands; data not shown). Immunoblot analysis of parotid and sub-

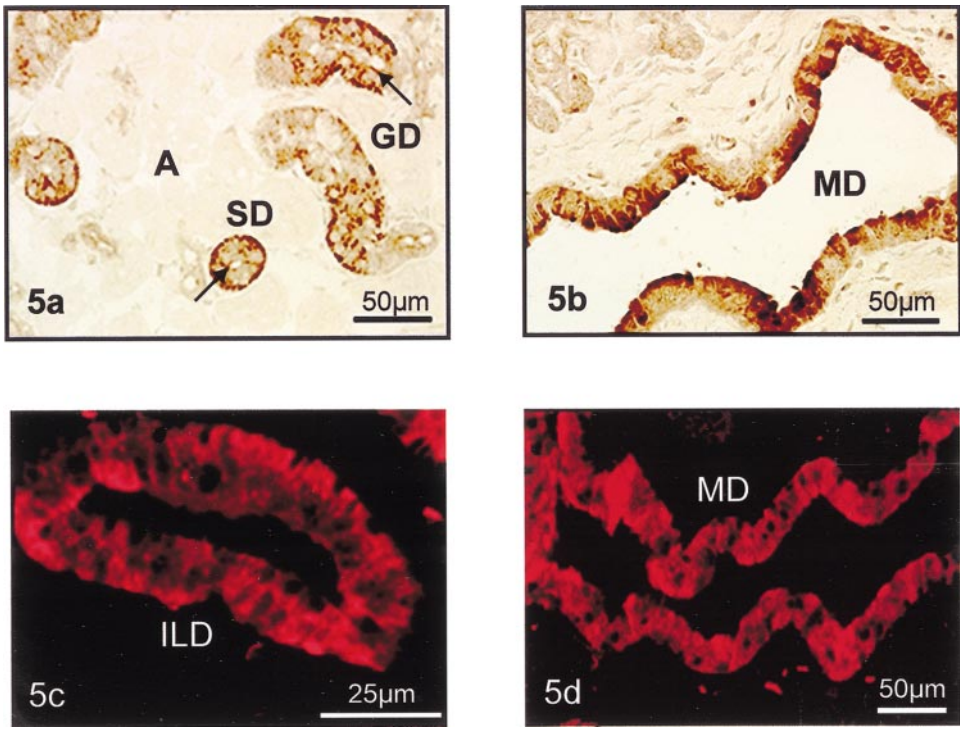

Fig. 5. Immunolocalization of NBC in rat submandibular gland with anti-(MPB-NBC3) antibody (1:400 dilution). Immunoperoxidase (*a* and *b*) or immunofluorescence light microscopy (*c* and *d*) was performed on 2% paraformaldehyde-75 mM lysine-10 mM sodium periodate-fixed cryosections. NBC immunoreactivity in submandibular acinar (A) cells, granular duct (GD) cells, and striated duct (SD) cells is shown. Arrows indicate striated duct cells labeled at both apical and basolateral membranes (*a*). NBC localization in main duct (MD) (*b*) and interlobular duct (ILD) (*c*) cells is shown. Immunofluorescence data on main duct cells confirmed the results obtained by immunoperoxidase (*d*). Representative images of 10 different sections from 5 animals are shown.

mandibular plasma membrane proteins with the AE2 antibody revealed protein bands at ~160 and ~180 kDa (Fig. 1*a*), exhibiting apparent molecular masses (M_r) corresponding to AE2a/b and to AE2c, respectively. The ~100-kDa and ~110-kDa bands correspond to the M_r of AE1 (15). Although these bands could in part be accounted for by residual erythrocytes in the gland tissue samples, their prominence may suggest expression of AE1 or the presence of a novel isoform. Indeed, a band of ~95 kDa has been reported in lung tissue that could represent a protein different from AE1 (21).

NBC. Both NBC antibodies labeled a ~130-kDa protein band (Fig. 1*b* and data not shown). A protein band labeled by anti-(MBP-NBC5) and anti-(MBP-NBC3) antisera of ~130 kDa has also been reported by our group in rat pancreas (39). This M_r of ~130 kDa is similar to the predicted molecular mass of mouse and human pancreatic NBC of ~121.5 kDa (GenBank AF020195.1 and AF011390.1) (1).

Immunolocalization of AE2 and NBC in Acini

Immunoperoxidase and immunofluorescence labeling showed a predominant AE2 and NBC localization at the plasma membrane, in accordance with the immunoblot data.

AE2. With the use of the anti AE2-CT antibody and epitope unmasking with SDS, a basolateral epitope was detected in parotid and submandibular acinar cells (Fig. 2*d*). These results are in agreement with an immunohistochemical study in rat submandibular gland (10) as well as with previous functional studies in rat parotid (20) and submandibular glands (8) and are also consistent with the current view of electrolyte transport in salivary acinar cells (41), according to which the basolaterally located Cl^-/HCO_3^- exchanger AE2 may, together with a Na^+/H^+ exchanger, control the intracellular pH and contribute to intracellular accumulation of Cl^- (22).

NBC. Interestingly, our results show that, in addition to AE2, parotid but not submandibular acinar cells also express NBC at their basolateral membranes, (Figs. 3*a* and 5*a*). This is in agreement with studies on rabbit submandibular acinar cells (9, 17), which did not find evidence for a Na^+-HCO_3^- cotransporter in these cells, but different from a study by Melvin et al. (19), who have provided no evidence for the presence of electrogenic Na^+-HCO_3^- cotransport in rat parotid acinar cells. However, the data of Melvin et al. could also not be fully explained by the current models of electrolyte transport in these cells, as transport was SITS insensitive but amiloride sensitive. In contrast, a Na^+-HCO_3^- cotransporter has been postulated for accumulation of HCO_3^- in sheep parotid acinar cells (24, 33), which may account for the ability of sheep parotid gland to produce a HCO_3^--rich primary fluid. However, without knowledge of the HCO_3^- concentration of the primary fluid, it is difficult to put forward a model that will account for both the various HCO_3^- secretion patterns and the ductal contribution on the HCO_3^- concentration in the final saliva. Moreover, the absence of NBC in submandibular acinar cells may indicate different fluid and electrolyte secretion mechanisms in the two glands.

Immunolocalization of AE2 and NBC in Ducts

Our results also demonstrate the absence or subthreshold level of expression of AE2 protein in both parotid and submandibular duct cells. These findings are in accordance with functional studies on isolated

rat parotid intralobular ducts (23) and with an immunohistochemical study on rat submandibular gland (10). In contrast, perfusion experiments in the main duct of rat submandibular gland have demonstrated the presence of luminal (8, 13) or of both luminal and basolateral Cl^-/HCO_3^- exchange activity (43, 46). The failure to detect AE2 in duct cells of rat salivary glands could either reflect epitope shielding or low abundance of the epitope but also absence of AE2, which would suggest that the major part of HCO_3^- transport does not take place via AE2. Considering the immunoblotting results obtained in the present study (Fig. 1*a*), it can obviously not be excluded that other AE isoforms (such as AE1 and/or AE3, or maybe a novel isoform) may be expressed in salivary duct cells.

On the basis of our studies, NBC could represent the relevant HCO_3^- transporter in both apical and basolateral membranes of parotid and submandibular glands. An electroneutral Na^+/HCO_3^- exchanger (mNBC3) has been recently cloned (25) that is insensitive to DIDS but sensitive to 5-(*N*-ethyl-*N*-isopropyl)amiloride. Although at this stage we cannot exclude that either the apical or basolateral immunolabeling could be accounted for by mNBC3 or a yet unknown novel isoform of NBC that may cross-react with our antibodies, it is rather unlikely that mNBC3 would represent the isoform expressed in salivary glands, because it was found to be uniquely expressed in skeletal muscle and heart but not in epithelial tissues, such as kidney, small intestine, or pancreas (25).

Our results provide evidence for a heterogeneous cellular distribution of HCO_3^- transporters in rat parotid and submandibular ducts (Figs. 3*a* and 5*a*). Basolateral NBC distribution was not consistent between duct segments but shifted to predominantly apical localization in main submandibular but not in parotid ducts, suggesting distinct HCO_3^- transport properties in the different duct segments of submandibular gland. Heterogeneity between submandibular and parotid glands has also been reported in previous studies on the distribution of vacuolar-type H^+-ATPase (V-ATPase) in salivary ducts (29, 30). Apical colocalization of V-ATPase and NBC could lead to HCO_3^- reabsorption rather than to HCO_3^- secretion in parotid duct cells, a possible explanation for the decrease of HCO_3^- concentration in the final fluid, compared with that of the primary fluid (8). In contrast, submandibular duct cells exhibit NBC at their apical membranes but no V-ATPase (29, 30), suggesting that the ducts may secrete HCO_3^- and contribute to the HCO_3^- concentration in the final fluid. Because no ductal cell AE2 expression was detected, the present study provides evidence that NBC likely plays a more important role in ductal HCO_3^- transport than previously believed.

We thank Alan Stuart-Tilley and Inge Naumann for excellent technical assistance.

This work was supported by National Institute of Diabetes and Digestive and Kidney Diseases Grants DK-43495 (to S. L. Alper) and DK-30344 (to W. F. Boron), by Cystic Fibrosis Core Center Grant P30-DK27651 (to M. F. Romero), and a Training Grant from the Deutsche Forschungsgemeinschaft (DFG) (SCHM 1297/1–1, to B. M. Schmitt). Research in F. Thévenod's laboratory is supported by DFG Grant Th 345/6–1.

Address for reprint requests and other correspondence: F. Thévenod, Department of Physiology, University of Saarland, Building 58, D-66421 Homburg/Saar, Germany (E-mail: frank.thevenod@med-rz.uni-sb.de).

Received 24 June 1999; accepted in final form 1 September 1999.

REFERENCES

1. **Abuladze, N., I. Lee, D. Newman, J. Hwang, K. Boorer, A. Pushkin, and I. Kurtz.** Molecular cloning, chromosomal localization, tissue distribution, and functional expression of the human pancreatic sodium bicarbonate cotransporter. *J. Biol. Chem*. 273: 17689–17695, 1998.
2. **Alper, S. L.** The band 3-related AE anion exchanger gene family. *Cell. Physiol. Biochem*. 4: 265–281, 1994.
3. **Alper, S. L., R. R. Kopito, S. M. Libresco, and H. F. Lodish.** Cloning and characterization of a murine band 3-related cDNA from kidney and from a lymphoid cell line. *J. Biol. Chem*. 263: 17092–17099, 1988.
4. **Alper, S. L., H. Rossmann, S. Wilhelm, A. K. Stuart-Tilley, B. E. Shmukler, and U. Seidler.** Expression of AE2 anion exchanger in mouse intestine. *Am. J. Physiol*. 277 (*Gastrointest. Liver Physiol*. 40): G321–G332, 1999.
5. **Alper, S. L., A. K. Stuart-Tilley, D. Biemesderfer, B. E. Shmuckler, and D. Brown.** Immunolocalization of AE2 anion exchanger in rat kidney. *Am. J. Physiol*. 273 (*Renal Physiol*. 42): F601–F614, 1997.
6. **Bradford, M. M.** A rapid and sensitive method for the quantitation of microgram quantities of protein utilizing the principle of protein-dye binding. *Anal. Biochem*. 72: 248–254, 1976.
7. **Brown, D., J. Lydon, M. McLaughlin, A. Stuart-Tilley, R. Tyszkowski, and S. Alper.** Antigen retrieval in cryostat tissue sections and cultured cells by treatment with sodium dodecyl sulfate (SDS). *Histochem. Cell Biol*. 105: 261–267, 1996.
8. **Cook, D. I., E. W. Van Lennep, M. L. Roberts, and J. A. Young.** Secretion by the major salivary glands. In: *Physiology of the Gastrointestinal Tract* (3rd ed.), edited by L. Johnson, J. Christensen, M. Jackson, E. Jacobson, and J. Walsh. New York: Raven, 1994, p. 1061–1117.
9. **Elliott, A. C., K. R. Lau, and P. D. Brown.** The effects of Na^+ replacement on intracellular pH and $[Ca^{2+}]$ in rabbit salivary gland acinar cells. *J. Physiol. (Lond.)* 444: 419–439, 1991.
10. **He, X., C. M. Tse, M. Donowitz, S. L. Alper, S. E. Gabriel, and B. J. Baum.** Polarized distribution of key membrane transport proteins in the rat submandibular gland. *Pflügers Arch*. 433: 260–268, 1996.
11. **Jensen, L. J., A. K. Stuart-Tilley, L. L. Peters, S. E. Lux, S. L. Alper, and S. Breton.** Immunolocalization of AE2 anion exchanger in rat and mouse epididymis. *Biol. Reprod*. 61: 973–980, 1999.
12. **Knauf, H., R. Lubcke, W. Kreutz, and W. Sachs.** Interrelationships of ion transport in rat submaxillary duct epithelium. *Am. J. Physiol*. 242 (*Renal Fluid Electrolyte Physiol*. 11): F132–F139, 1982.
13. **Knauf, H., P. Röttger, U. Wais, and K. Baumann.** On the regulatory handling of Na^+, K^+ and H^+ transport by the rat salivary epithelium. *Fortschr. Zool*. 23: 307–321, 1975.
14. **Kopito, R. R., B. S. Lee, D. M. Simmons, A. E. Lindsey, C. W. Morgens, and K. Schneider.** Regulation of intracellular pH by a neuronal homolog of the erythrocyte anion exchanger. *Cell* 59: 927–937, 1989.
15. **Kopito, R. R., and H. F. Lodish.** Primary structure and transmembrane orientation of the murine anion exchanger protein. *Nature* 316: 234–238, 1985.
16. **Kudrycki, K. E., P. R. Newman, and G. E. Shull.** cDNA cloning and tissue distribution of mRNAs for two proteins that are related to the band 3 Cl^-/HCO_3^- exchanger. *J. Biol. Chem*. 265: 462–471, 1990.
17. **Lau, K. R., A. C. Elliott, and P. D. Brown.** Acetylcholine-induced intracellular acidosis in rabbit salivary gland acinar cells. *Am. J. Physiol*. 256 (*Cell Physiol*. 25): C288–C295, 1989.

18. **McLean, I. W., and P. F. Nakane.** Periodate-lysine paraformaldehyde fixative: a new fixative for immunoelectron microscopy. *J. Histochem. Cytochem.* 22: 1077–1083, 1974.
19. **Melvin, J. E., A. Moran, and R. J. Turner.** The role of HCO_3^- and Na^+/H^+ exchange in the response of rat parotid and acinar cells to muscarinic stimulation. *J. Biol. Chem.* 263: 19564–19569, 1988.
20. **Melvin, J. E., and R. J. Turner.** Cl^- fluxes related to fluid secretion by the rat parotid: involvement of Cl^--HCO_3^- exchange. *Am. J. Physiol.* 262 (*Gastrointest. Liver Physiol.* 25): G393–G398, 1992.
21. **Noviz-Grayck, E., C. A. Piantadosi, J. van Adelsberg, S. L. Alper, and Y.-C. T. Huang.** Protection of perfused lung from oxidant injury by inhibitors of anion exchanger. *Am. J. Physiol.* 273 (*Lung Cell. Mol. Physiol.* 17): L296–L304, 1997.
22. **Park, K., J. A. Olschowka, L. A. Richardson, C. Bookstein, E. B. Chang, and J. E. Melvin.** Expression of multiple Na^+/H^+ exchanger isoforms in rat parotid acinar and ductal cells. *Am. J. Physiol.* 276 (*Gastrointest. Liver Physiol.* 39): G470–G478, 1999.
23. **Paulais, M., E. J. Cragoe, Jr., and R. J. Turner.** Ion transport in rat parotid intralobular striated ducts. *Am. J. Physiol.* 266 (*Cell Physiol.* 35): C1594–C1602, 1994.
24. **Poronnik, P., S. Y. Schumann, and D. I. Cook.** HCO_3^--dependent ACh-activated Na^+ influx in sheep parotid secretory end pieces. *Pflügers Arch.* 429: 852–858, 1995.
25. **Pushkin, A., N. Abuladze, I. Lee, D. Newman, J. Hwang, and I. Kurtz.** Cloning, tissue distribution, genomic organization, and functional characterization of NBC3, a new member of the sodium bicarbonate cotransporter family. *J. Biol. Chem.* 274: 16569–16575, 1999.
26. **Romero, M. F., and W. F. Boron.** Electrogenic Na^+/HCO_3^- cotransporters: expression, cloning and physiology. *Ann. Rev. Physiol.* 61: 699–723, 1999.
27. **Romero, M. F., M. A. Hediger, E. L. Boulpaep, and W. F. Boron.** Expression, cloning and characterization of a renal electrogenic Na^+/HCO_3^--cotransporter. *Nature* 387: 409–413, 1997.
28. **Romero, M. F., P. Fong, U. V. Berger, M. A. Hediger, and W. F. Boron.** Cloning and functional expression of rNBC, an electrogenic Na^+-HCO_3^- cotransporter from rat kidney. *Am. J. Physiol.* 274 (*Renal Physiol.* 43): F425–F432, 1998.
29. **Roussa, E., and F. Thévenod.** Distribution of V-ATPase in rat salivary glands. *Eur. J. Morphol.* 36, *Suppl.*: 147–152, 1998.
30. **Roussa, E., F. Thévenod, I. Sabolic, C. M. Herak-Kramberger, W. Nastainczyk, R. Bock, and I. Schulz.** Immunolocalization of vacuolar-type H^+-ATPase in rat submandibular gland and adaptive changes induced by acid-base disturbances. *J. Histochem. Cytochem.* 46: 91–100, 1998.
31. **Schmitt, B. M., D. Biemesderfer, M. F. Romero, E. L. Boulpaep, and W. F. Boron.** Immunolocalization of the electrogenic Na^+/HCO_3^- cotransporter in Mammalian and amphibian kidney. *Am. J. Physiol.* 276 (*Renal Physiol.* 45): F27–F38, 1999.
32. **Shackleford, J. M., and L. H. Schneyer.** Ultrastructural aspects of the main excretory duct of rat submandibular gland. *Anat. Rec.* 169: 679–696, 1971.
33. **Steward, M. C., P. Poronnik, and D. I. Cook.** Bicarbonate transport in sheep parotid secretory cells. *J Physiol. (Lond.)* 494: 819–830, 1996.
34. **Stuart-Tilley A., C. Sardet, J. Pouyssegur, M. A. Schwartz, D. Brown, and S. L. Alper.** Immunolocalization of anion exchanger AE2 and cation exchanger NHE-1 in distinct adjacent cells of gastric mucosa. *Am. J. Physiol.* 266 (*Cell Physiol.* 35): C559–C568, 1994.
35. **Stuart-Tilley, A. K., B. E. Shmuckler, D. Brown, and S. L. Alper.** Immunolocalization and tissue specific splicing of AE2 anion exchanger in mouse kidney. *J. Am. Soc. Nephrol.* 9: 946–959, 1998.
36. **Tamarin, A. L., and M. Sreebny.** The rat submaxillary salivary gland. A correlative study by light and electron microscopy. *J. Morphol.* 117: 295–352, 1965.
37. **Thaysen, J. H., N. A. Thorn, and I. L. Schwartz.** Excretion of sodium, potassium, chloride and carbon dioxide in human parotid saliva. *Am. J. Physiol.* 178: 155–159, 1954.
38. **Thévenod, F., I. Anderie, and I. Schulz.** Monoclonal antibodies against MDR1 P-glycoprotein inhibit chloride conductance and label a 65-kD protein in pancreatic zymogen granule membranes. *J. Biol. Chem.* 269: 24410–24417, 1994.
39. **Thévenod, F., E. Roussa, B. M. Schmitt, and M. F. Romero.** Cloning and immunolocalization of a rat pancreatic Na^+ bicarbonate cotransporter. *Biochem. Biophys. Res. Commun.* 264: 291–298, 1999.
40. **Thévenod, F., and I. Schulz.** H^+-dependent calcium uptake into an IP3-sensitive calcium pool from rat parotid gland. *Am. J. Physiol.* 255 (*Gastrointest. Liver Physiol.* 18): G429–G440, 1988.
41. **Turner, R. J.** Mechanisms of fluid secretion by salivary glands. *Ann. NY Acad. Sci.* 694: 24–35, 1993.
42. **Vázquez, J. J., M. Vázquez, M. A. Idoate, L. Montuenga, E. Martínez-Ansó, J. E. Castillo, N. García, J. F. Medina, and J. Prieto.** Anion exchanger immunoreactivity in human salivary glands in health and Sjögren's syndrome. *Am. J. Pathol.* 146: 1422–1432, 1995.
43. **Xu, X., H. Zhao, J. Diaz, and S. Muallem.** Regulation of $[Na^+]_i$ in resting and stimulated submandibular salivary ducts. *J. Biol. Chem.* 270: 19606–19612, 1995.
44. **Yannoukakos, D., A. Stuart-Tilley, H. A. Fernandez, P. Fey, G. Duyk, and S. L. Alper.** Molecular cloning, expression, and chromosomal localization of two isoforms of the AE3 anion exchanger from human heart. *Circ Res.* 75: 603–614, 1994.
45. **Young, J. A., and E. W. Van Lennep.** *The Morphology of Salivary Glands.* New York: Academic, 1978.
46. **Zhao, H., X. Xu, J. Diaz, and S. Muallem.** Na^+, K^+, and H^+/HCO_3^- transport in submandibular salivary ducts. *J. Biol. Chem.* 270: 19599–19605, 1995.